Toward high-efficiency solar upconversion with plasmonic nanostructures

2012 J. Opt. 14 024008

(http://iopscience.iop.org/2040-8986/14/2/024008)

IOP Publishing Journal of Optics

J. Opt. **14** (2012) 024008 (7pp) doi:10.1088/2040-8978/14/2/024008

Toward high-efficiency solar upconversion with plasmonic nanostructures

Ashwin C Atre[1], Aitzol García-Etxarri[1,2], Hadiseh Alaeian[3] and Jennifer A Dionne[1]

[1] Department of Materials Science, Stanford University, Stanford, CA 94305, USA
[2] IKERBASQUE, Basque Foundation for Science, 48011, Bilbao, Spain
[3] Department of Electrical Engineering, Stanford University, Stanford, CA 94305, USA

E-mail: aatre@stanford.edu and jdionne@stanford.edu

Received 31 August 2011, accepted for publication 23 September 2011
Published 12 January 2012
Online at stacks.iop.org/JOpt/14/024008

Abstract
Upconversion of sub-bandgap photons can increase the maximum efficiency of a single-junction solar cell from 30% to over 44%. However, upconverting materials often have small absorption cross-sections and poor radiative recombination efficiencies that limit their utility in solar applications. Here, we show that the efficiency of upconversion can be substantially enhanced with a suitably designed plasmonic nanostructure. The structure consists of a spherical nanocrescent composed of an upconverter-doped dielectric core and a crescent-shaped metallic shell. Using numerical techniques, we calculate a greater than 10-fold absorption enhancement for a broad range of sub-bandgap wavelengths throughout the entire upconverting core. Further, this nanocrescent enables a 100-fold increase in above-bandgap power emission toward the solar cell. Our results provide a framework for achieving low-power solar upconversion, potentially enabling a single-junction solar cell with an efficiency exceeding the Shockley–Queisser limit.

Keywords: solar cells, upconversion, plasmonics, nanocrescents

(Some figures in this article are in colour only in the electronic version)

Efficient solar energy harvesting relies on the precise control of light–matter interactions. Whether photons are used for catalyzing chemical reactions or separating charges to produce electricity, the efficiency of all energy conversion processes is regulated by light absorption in the active materials. To improve the interaction of solar photons with light absorbing media, metallic nanostructures can be used. Illumination of these nanostructures excites coherent oscillations of the conduction electrons, known as surface plasmons. Plasmons not only create substantial near-field intensities, but also modify the absorption and scattering cross-section of the nanostructure beyond its physical size.

Recently, plasmonic materials have gained considerable attention for their ability to manipulate light in solar cells, substantially increasing the absorption of above-bandgap photons [1]. By patterning the back contact of a solar cell with subwavelength metallic features, absorption can be more than doubled via the coupling of incident light into surface plasmon polaritons [2, 3]. Alternatively, based on the excitation of localized surface plasmon polaritons, metallic nanoparticles can be used to preferentially scatter light into the active material of the device [4–6], or to enhance the local electromagnetic field in this region [7, 8].

However, even if a solar cell were able to absorb all above-bandgap light, its efficiency would be significantly limited by the solar power lost due to the transmission of sub-bandgap photons. For example, a solar cell with a bandgap of 1.8 eV wastes nearly 54% of the incident solar power due to sub-bandgap transmission. To reduce transmission losses, upconversion based on sequential multi-photon absorption has been proposed [9]. Placed behind the solar cell, an upconverter transforms transmitted low-energy photons to higher-energy, above-bandgap photons that can then be absorbed by the solar cell (see figure 1(a)). Because the upconverter is electrically isolated from the active cell above, the upconverter is able to harvest the power contained in sub-bandgap solar photons without reducing the above-bandgap cell performance. Prior calculations have shown that the efficiency of an ideal

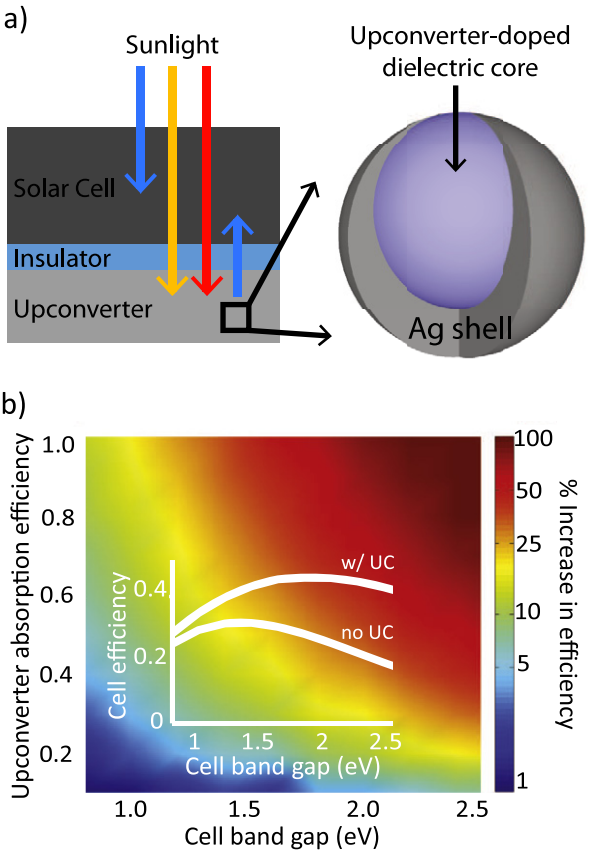

Figure 1. (a) Schematic diagram of the solar cell–upconverter system. Above-bandgap light is absorbed by the solar cell, while sub-bandgap light is absorbed in the upconverter layer. The upconverter consists of metal–dielectric core–shell nanocrescents, in which the core is doped with the upconverting material. (b) An upconverter (UC) can significantly increase the efficiency of an ideal single-junction solar cell. This relative increase is greatest when the upconverter absorption efficiency and cell bandgap are high. The inset shows the absolute efficiency for an ideal solar cell both with and without an ideal upconverter.

single-junction device under non-concentrated sunlight can be improved from 30% to over 44% by addition of an ideal upconverter [9–11].

While low-power solar upconversion has been demonstrated [12, 13], efficient upconversion with non-concentrated sunlight has not been achieved. Preventing the successful implementation of upconversion in a photovoltaic device have been the low absorption efficiencies and high non-radiative recombination rates of upconverting systems [14–16]. In the same way that plasmonic materials can be used to improve the above-bandgap absorption of a solar cell, such nanostructures can be tailored to increase the interaction of sub-bandgap photons with an upconverter. Indeed, plasmonic enhancement of upconverted fluorescence over narrow spectral bandwidths has been demonstrated, but high-power, coherent excitation was employed [17–21].

Here, we propose a unique plasmonic nanoantenna for enhancing solar upconversion over broad spectral and spatial regions. The structure consists of a metallic nanoshell with an offset upconverter-doped dielectric core, referred to as a nanocrescent (see figure 1(a)). This structure exhibits strong electromagnetic field concentration in the dielectric core that can be spectrally tuned with the geometric parameters of the system. Recent theoretical work has demonstrated the capabilities of related structures for efficient light harvesting across the entire visible spectrum [22]. Further, nanocrescents and 'nanocups' have been synthesized with a range of sizes (from 30 to 200 nm in diameter) [23], and experimental results indicate strong surface-enhanced Raman scattering (SERS) [24] as well as tunable scattering [25].

In this paper we quantify the theoretical limits of upconverter-enhanced photovoltaics and explore the upconverter-doped nanocrescent as a plasmonic geometry to significantly enhance both the upconverter absorption of sub-bandgap photons and subsequent emission of above-bandgap photons. We show that the spherical nanocrescent serves as both a sub-bandgap receiving antenna and as an above-bandgap antenna for emission. Via it's large and broad near-field intensity enhancements, this plasmonic geometry could substantially improve the performance of upconverter systems, potentially increasing the power conversion efficiency of single-junction solar cells beyond the Shockley–Queisser limit.

In the context of upconversion-enhanced photovoltaics, it is important to quantify the potential improvements possible in utilizing sub-bandgap photons. The efficiency of an upconverter-enhanced single junction solar cell can be determined using a detailed balance approach. The method relates the overall solar cell current density to the difference between the absorbed and emitted photon flux densities. Details of the cell–upconverter model can be found in [9, 11]. Briefly, the upconverter is modeled as a light emitting diode (LED) emitting photons with an energy equal to the solar cell bandgap. This LED is driven into forward bias by two sequential low-energy photon absorption events. Any photons not absorbed by the single-junction cell are transmitted to the upconverter and can be used to produce additional photocurrent.

Figure 1(b) illustrates the photovoltaic efficiency improvement that can be achieved by adding an upconverter to an ideal single-junction cell. The results are normalized to a cell without an upconverting layer. In the absence of an upconverter, our cell efficiency calculations perfectly match the Shockley–Queisser limit [26], as seen in the inset. By adding an upconverter, the solar cell efficiency can be dramatically increased. As the figure illustrates, efficiency enhancements are seen for all cell bandgaps, even if the upconverter is not ideal. To span the characteristics of most upconverters—including lanthanoids [27, 28], metal–ligand complexes [15], and quantum dots [29], we consider upconverter absorption efficiencies ranging from 0.1 to 1. As expected, the relative increase in efficiency due to the upconverter is highest when the upconverter absorption efficiency is maximized and the cell bandgap is highest.

In the limit of an ideal cell and an ideal upconverter, the peak device efficiency increases from 30% to 44.4%—an increase in single-junction solar cell performance of nearly

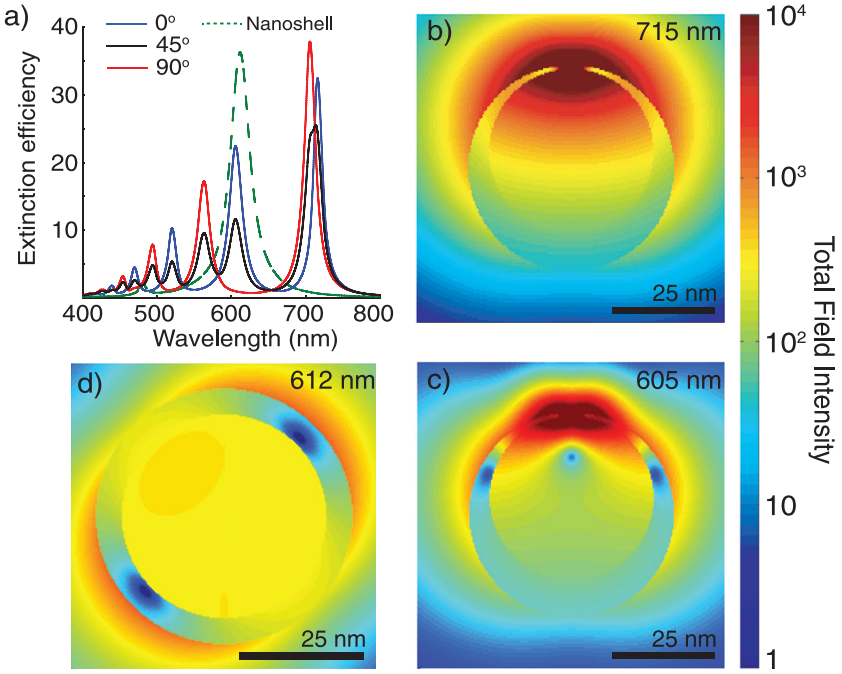

Figure 2. Optical properties of a Ag–dielectric spherical nanocrescent. (a) Extinction efficiency (cross-section normalized by the physical cross-sectional area) for various crescent orientations. The dashed line is the extinction cross-section of a symmetric nanoshell. Normalized electric field intensity distributions of the crescent at (b) 715 nm, the lowest-energy resonance for normal incidence (0°), and (c) 605 nm, the second order resonance. (d) The electric field intensity distribution for the symmetric nanoshell at 612 nm is presented for comparison. The outer diameter of the crescent and nanoshell is 50 nm, while the inner dielectric core has an index of 1.47 and a diameter of 40 nm. The gap between the tips of the crescent is 5 nm.

70% (see the inset of figure 1(b)). Since the upconverter allows utilization of sub-bandgap photons, the optimal cell bandgap for a cell–upconverter system is actually blue-shifted from 1.1 to 1.8 eV. Interestingly, this bandgap is characteristic of numerous thin-film solar cells, including amorphous Si, dye-sensitized TiO_2, and organic photovoltaics.

As seen in the figure, an increase in the upconverter absorption efficiency causes a significant increase in the solar cell efficiency. Because the cell and upconverter are electrically isolated, addition of an upconverter always improves cell performance, even for poorly performing upconverters. However, to maximize photovoltaic power conversion, it is essential to optimize performance of the upconverter—including enhancements in the absorption efficiency of below-bandgap light, as well as the subsequent emission efficiency of upconverted (above-bandgap) light. In the following text, we describe the spherical nanocrescent as a plasmonic geometry that simultaneously enables high upconverter absorption and emission efficiencies, tunable across a broad spectral range.

Due to the broadband and intense field enhancements associated with spherical metal–dielectric nanocrescents, we anticipate that this geometry will dramatically enhance the upconversion process. To explore this hypothesis, we consider a realistic spherical silver nanocrescent with an upconverter-doped dielectric core. Figure 1(a) illustrates the selected upconverter-doped crescent geometry. This nanostructure is especially appealing because the metallic crescent shell could be easily formed around upconverter-doped dielectric nanoparticles, effectively encapsulating the upconverter system within the plasmonic shell. A closely related geometry is the symmetric core–shell particle, the properties of which will be compared throughout the following discussion.

The crescent considered here consists of an outer Ag shell with a diameter of 50 nm; an inner dielectric core with an index of 1.47 and diameter of 40 nm, displaced by 4 nm from the center of the outer sphere; and a circular gap in the tips with a 5 nm diameter, resulting in a tip thickness of approximately 1 nm. The size of the crescent was selected to have resonant features most compatible with the optimum upconverter-enhanced cell bandgap of 1.8 eV, as identified in the previous analysis. For the following discussion, light incident at 0° is defined with the wavevector parallel to the rotational axis, while the polarization of the electric and magnetic fields is irrelevant due to the symmetry of the particle. Light incident at 90° is defined with the wavevector orthogonal to the axis of rotation and the electric field parallel to that axis.

The optical properties of dielectric–metal core–shell nanocrescents and nanoshells are calculated using the boundary element method [30, 31], with the optical properties of Ag adopted from empirical data [32]. Figure 2(a) plots the extinction efficiency of the nanocrescent for different orientations of incident light. For comparison, the extinction efficiency of the same sized symmetric core–shell spherical nanoparticle is plotted as well. The figure clearly illustrates the strong, broadband resonant characteristics of the crescent

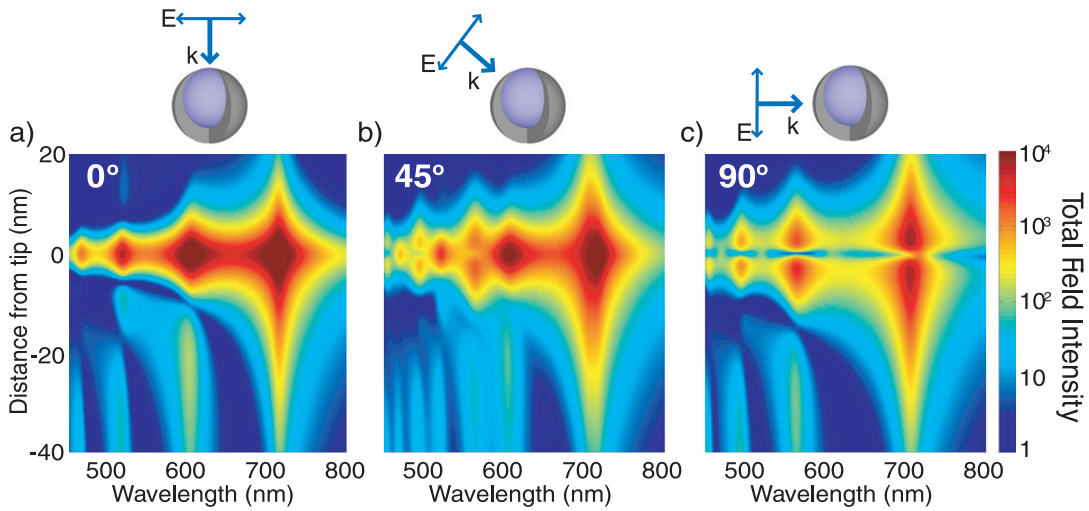

Figure 3. (a) Spectral and spatial maps of the normalized electric field intensity showing large enhancements throughout the entire inner core of the crescent, spanning from −40 nm at the back to 0 nm at the tips. The enhancements occur regardless of crescent orientation: (a) 0°, (b) 45°, and (c) 90°.

nanostructure, as well as the non-ideal, relatively narrowband response of the symmetric nanoshell structure. The separate peaks in the crescent spectra correspond to the various modes of the system [25, 33]. For light incident at 45°, all optically active modes of the system are excited. At the peak wavelength of 715 nm, the cross-section is 25 times the physical cross-section of the particle. Accordingly, only a small concentration of crescents is needed to harvest the incident sub-bandgap light.

In an actual solar cell–upconverter device, the strong lowest order resonance of the crescent will enhance the absorption of sub-bandgap photons by the upconverter located in the crescent core. This makes the present crescent geometry ideal for use with a solar cell with a bandgap of approximately 1.8 eV (λ_g = 690 nm). Though not shown, variation of the crescent geometry and core index would allow this resonance to be tuned throughout the visible and near infrared, as explored previously [34].

The large electric field intensity associated with this lowest order resonance, plotted in figure 2(b), illustrates the strong potential of this structure for enhancing the absorption of an upconverting system located within the core. For the lowest order mode at 715 nm, the electric field intensity peaks at nearly 10^5 close to the tips, a feature used previously for SERS applications [24]. More importantly for upconversion, the intensity remains greater than 10^2 throughout the entire core of the particle for this wavelength, suggesting an effective upconverter absorption enhancement of greater than 10^2. Interestingly, a portion of the hotspot volume is located outside the crescent, indicating that upconverting material just outside the crescent would also experience enhanced fields and thus enhanced absorption.

The resonance at 605 nm, which will be used for enhanced above-bandgap emission, is shown in figure 2(c). Much like the lowest order resonance, this mode is characterized by a spectrally and spatially broad response.

For comparison, the symmetric nanoshell exhibits near-field intensities just above 10^2 in the dielectric core at the peak extinction wavelength of 612 nm (see figure 2(d)). Furthermore, the highest intensity achieved with the nanoshell is two orders of magnitude lower than that obtained near the tips of the nanocrescent. Equally important is the fact that the nanoshell only supports a single strong resonance, precluding broadband enhancement of the spectrally dissimilar absorption and emission events of the upconverter. The crescent, on the other hand, exhibits multiple resonances which can be tuned to overlap with the upconverter absorption and emission wavelengths. Notably, the lowest order resonance has a full-width at half-maximum of almost 30 nm, corresponding to the absorption bandwidth of the best upconverting systems [15].

For the nanocrescent structure, normalized near-field intensity spectra are plotted in figure 3 as a function of position along the crescent central axis for various crescent orientations. In these plots the inner core of the crescent, which contains the upconverting system, is located between 0 and −40 nm. For normal incidence, shown in figure 3(a), electric field intensities greater than 50 are calculated for a 50 nm bandwidth around 715 nm over nearly the entire inner core. This broad spectral and spatial response of the spherical nanocrescent has yet to be experimentally demonstrated, but is ideal for enhancing upconverter absorption.

Figure 3(c) plots the near-field intensity spectra for the orthogonal polarization of incident light. Even though the local field enhancement at the tips is reduced due to the symmetry of the modes with respect to the central axis, the strength and spectral breadth of the field intensity throughout the inner core is maintained. Correspondingly, even an intermediate incidence, shown in figure 3(b), exhibits large field enhancement throughout the inner core.

The above results illustrate that this nanocrescent geometry acts as a very efficient nanoantenna for concentrating sub-bandgap light. Notably, this geometry promises

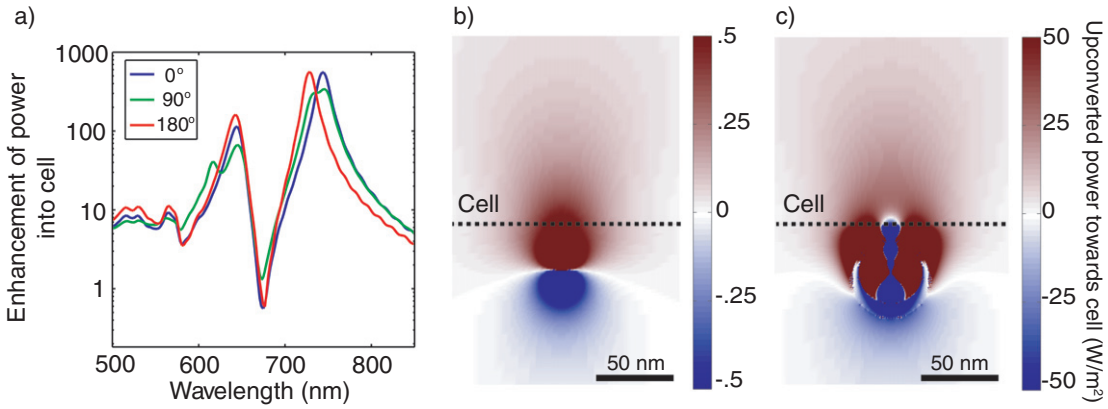

Figure 4. Simulated enhancement of upconverted fluorescence from an upconverter located at the center of the crescent dielectric core, normalized to an upconverter without the nanocrescent. (a) Enhancement of power flowing into a dielectric slab, here assumed to be Si, for various crescent orientations: tips oriented toward the slab (0°), away from the slab (180°), or at an intermediate position. At a wavelength of 644 nm, power flow into the cell (positive in the vertical direction) is enhanced by more than 100 times with the crescent (c), relative to an emitter without the crescent (b). Note that the scale of the colormap in (c) is increased by two orders of magnitude.

upconversion absorption enhancement across a broad spatial and spectral range of at least 10^2. Of course, efficient upconversion also requires strong emission of upconverted light back toward the solar cell. Aside from producing high local electromagnetic fields that can enhance absorption, surface plasmons also modify the emission rate and quantum efficiency of an emitter via the Purcell effect [35, 36]. In the following discussion, we determine the efficiency with which upconverted photons are emitted from the crescent and enter the active solar cell material.

To accurately study crescent–cell interactions, we employ three-dimensional full-field finite-difference time-domain simulations of a spherical nanocrescent near a dielectric slab, representing the solar cell and assumed to have the optical properties of Si. First, we calculate the response of an arbitrarily oriented point dipole (representing the upconverter emission) located approximately 30 nm from the Si and centered within the crescent dielectric core. This emission is then compared to the emission of a dipole without a plasmonic nanocrescent. In each case, the dipole is located the same distance from the Si surface. Also, the surrounding medium is assumed to be a dielectric with refractive index $n = 1.47$, as before.

By comparing the total power flux into the solar cell from the dipole emitter both with and without the crescent, we determine a conservative measure of the upconverted fluorescence emission enhancement and subsequent absorption in the solar cell. It is important to note that this above-bandgap power absorbed by the solar cell originates from sub-bandgap photons, and therefore will always result in an increase in photocurrent relative to a cell without an upconverter. The crescent enhancement of upconverted power flowing into the cell is shown in figure 4(a) for various crescent orientations. As seen, the orientation of the crescent has relatively little effect on the power enhancements due to the crescent resonance. Whether the tips point toward the cell (0°), parallel to the cell (90°), or away from the cell (180°), power enhancements in excess of 100 can be seen for the first and second order crescent resonances. The fact that the enhancement is nearly independent of crescent orientation is promising for practical applications of this concept, in which randomly oriented crescents would be much easier to incorporate into a real device. Note that the slight red shift of the peaks in this spectrum relative to the cross-sections of figure 3 arises from the local refractive index, here modified by the presence of the Si.

For solar upconversion applications, it is crucial to enhance both the absorption and fluorescence of an emitter. Assuming our upconverter emits at an energy close to the bandgap of our cell (here assumed to be 1.8 eV, characteristic of amorphous Si), enhanced emission at wavelengths shorter than 690 nm is desired. As figure 4(a) illustrates, the enhancement of power into the cell is greater than 10 for wavelengths between 600 and 650 nm. For an upconverter fluorescing at a wavelength of 644 nm within a nanocrescent, approximately 100 times more power will be transmitted to the cell than if the upconverter were simply fluorescing near the cell without the crescent.

This concept is illustrated in the near-field maps of the power flow in the direction of the cell at 644 nm in figures 4(b) and (c). For brevity, we only include maps for a dipole oriented parallel to the cell surface and for a crescent whose tips point toward the cell; randomly oriented dipoles yield similar results, as demonstrated by figure 4(a). The enhancement due to the presence of the crescent requires the color scale to increase by two orders of magnitude, demonstrating strong emission enhancement at this second order crescent resonance.

Overall, the upconversion process takes advantage of the electromagnetic response of the crescents twice. First the crescent acts as a receiving antenna, inducing very high near fields that enhance the absorption efficiency of the upconverter. Then, the high-energy photons emitted by the upconverter are efficiently re-radiated toward the cell, exploiting the radiative properties of the crescent as an emitting antenna. This process is related to the working principles of SERS [37], though here the absorption and emission are enhanced at very

different energies, with the emission occurring anti-Stokes, or blue-shifted, relative to the absorption. For the specific geometry of crescent explored herein, we predict an absorption enhancement of approximately 10^2 around 715 nm and an emission enhancement of approximately 10^2 around 644 nm for a randomly oriented upconverter located at the center of the crescent. It is important to note that the enhancements of absorption and emission are orders of magnitude greater for an upconverter located near the tips of the crescent. Furthermore, these resonances can be tuned through geometric and refractive index variation of the crescents for application to arbitrary photovoltaic systems.

In summary, we have investigated the potential of harvesting sub-bandgap light using an upconverter-doped plasmonic nanocrescent. Our numerical calculations demonstrate that these plasmonic nanoantennas can effectively localize and enhance the electric field in the upconverter-doped core by a factor of 100. Further, the radiative properties of this antenna in the vicinity of a photovoltaic cell is independent of crescent orientation and strongly directed into the cell. In fact, the emission efficiency of upconverted fluorescence can be enhanced by a factor of 100 with a suitably designed plasmonic crescent. With a solar cell incorporating optimized crescent-enhanced upconverters, more light across a broader spectrum will be absorbed than previously possible. Ultimately, such nanostructured materials will enable low-cost single-junction solar cells with efficiencies exceeding the Shockley–Queisser limit.

Acknowledgments

ACA acknowledges support from the Robert L and Audrey S Hancock Stanford Graduate Fellowship. AGE was supported by 'Programa de perfeccionamiento de doctores y doctoras en el extranjero del Departamento de Educación, Universidades e Investigación del Gobierno Vasco'. JAD acknowledges support from a Stanford Terman Fellowship, a Robert N Noyce Family Faculty Fellowship, and Hellman Faculty Scholar Funds. We also acknowledge insightful scientific discussions with Sassan Sheikholeslami.

References

[1] Atwater H A and Polman A 2010 Plasmonics for improved photovoltaic devices *Nature Mater.* **9** 205–13
[2] Ferry V E, Sweatlock L A, Pacifici D and Atwater H A 2008 Plasmonic nanostructure design for efficient light coupling into solar cells *Nano Lett.* **8** 4391–7
[3] Tvingstedt K, Persson N-K, Inganäs O, Rahachou A and Zozoulenko I V 2007 Surface plasmon increase absorption in polymer photovoltaic cells *Appl. Phys. Lett.* **91** 113514
[4] Pillai S, Catchpole K R, Trupke T and Green M A 2007 Surface plasmon enhanced silicon solar cells *J. Appl. Phys.* **101** 093105
[5] Catchpole K R and Polman A 2008 Design principles for particle plasmon enhanced solar cells *Appl. Phys. Lett.* **93** 191113
[6] Nakayama K, Tanabe K and Atwater H A 2008 Plasmonic nanoparticle enhanced light absorption in GaAs solar cells *Appl. Phys. Lett.* **93** 121904
[7] Kim S S, Na S I, Jo J, Kim D Y and Nah Y C 2008 Plasmon enhanced performance of organic solar cells using electrodeposited Ag nanoparticles *Appl. Phys. Lett.* **93** 073307
[8] Westphalen M, Kreibig U, Rostalski J, Lüth H and Meissner D 2000 Metal cluster enhanced organic solar cells *Sol. Energy Mater. Sol. Cells* **61** 97–105
[9] Trupke T, Green M A and Würfel P 2002 Improving solar cell efficiencies by up-conversion of sub-band-gap light *J. Appl. Phys.* **92** 4117
[10] Badescu V 2008 An extended model for upconversion in solar cells *J. Appl. Phys.* **104** 113120
[11] Atre A C and Dionne J A 2011 Realistic upconverter-enhanced solar cells with non-ideal absorption and recombination efficiencies *J. Appl. Phys.* **110** 034505
[12] Baluschev S, Miteva T, Yakutkin V, Nelles G, Yasuda A and Wegner G 2006 Up-conversion fluorescence: noncoherent excitation by sunlight *Phys. Rev. Lett.* **97** 143903
[13] Islangulov R R, Lott J, Weder C and Castellano F 2007 Noncoherent low-power upconversion in solid polymer films *J. Am. Chem. Soc.* **129** 12652
[14] Pollnau M, Gamelin D R, Lüthi S R, Güdel H U and Hehlen M P 2000 Power dependence of upconversion luminescence in lanthanide and transition-metal-ion systems *Phys. Rev.* B **61** 3337–46
[15] Singh-Rachford T N and Castellano F 2010 Photon upconversion based on sensitized triplet–triplet annihilation *Coord. Chem. Rev.* **254** 2560–73
[16] Baluschev S, Yakutkin V, Wegner G, Minch B, Miteva T, Nelles G and Yasuda A 2007 Two pathways for photon upconversion in model organic compound systems *J. Appl. Phys.* **101** 023101
[17] Baluschev S, Yu F, Miteva T, Ahl S, Yasuda A, Nelles G, Knoll W and Wegner G 2005 Metal-enhanced up-conversion fluorescence: effective triplet–triplet annihilation near silver surface *Nano Lett.* **5** 2482–4
[18] Aisaka T, Fujii M and Hayashi S 2008 Enhancement of upconversion luminescence of Er doped Al_2O_3 films by Ag island films *Appl. Phys. Lett.* **92** 132105
[19] Zhang H, Li Y, Ivanov I A, Qu Y, Huang Y and Duan X 2010 Plasmonic modulation of the upconversion fluorescence in $NaYF_4$:Yb/Tm hexaplate nanocrystals using gold nanoparticles or nanoshells *Angew. Chem.* **49** 2865–8
[20] Schietinger S, Aichele T, Wang H-Q, Nann T and Benson O 2010 Plasmon-enhanced upconversion in single $NaYF_4$:Yb3 + /Er3 + codoped nanocrystals *Nano Lett.* **10** 134–8
[21] Hallermann F, Rockstuhl C, Fahr S, Seifert G, Wackerow S, Graener H, Plessen G and Lederer F 2008 On the use of localized plasmon polaritons in solar cells *Phys. Status Solidi* a **205** 2844–61
[22] Aubry A, Lei D Y, Fernandez-Dominguez A I, Sonnefraud Y, Maier S A and Pendry J B 2010 Plasmonic light-harvesting devices over the whole visible spectrum *Nano Lett.* **10** 2574–9
[23] Britt Lassiter J, Knight M W, Mirin N A and Halas N J 2009 Reshaping the plasmonic properties of an individual nanoparticle *Nano Lett.* **9** 4326–32
[24] Lu Y, Liu G, Kim J, Mejia Y and Lee L 2005 Nanophotonic crescent moon structures with sharp edge for ultrasensitive biomolecular detection by local electromagnetic field enhancement effect *Nano Lett.* **5** 119–24
[25] Mirin N A and Halas N J 2009 Light-bending nanoparticles *Nano Lett.* **9** 1255–9
[26] Shockley W and Queisser H J 1961 Detailed balance limit of efficiency of pn junction solar cells *J. Appl. Phys.* **32** 510
[27] de Wild J, Meijerink A, Rath J K, van Sark W G J H M and Schropp R E I 2010 Towards upconversion for amorphous silicon solar cells *Sol. Energy Mater. Sol. Cells* **94** 1919–22

[28] Gamelin D and Güdel H 2001 Upconversion processes in transition metal and rare earth metal systems *Transition Metal and Rare Earth Compounds. Topics in Current Chemistry* (Berlin; Heidelberg: Springer) p 214
[29] Poles E, Selmarten D C, Mićić O I and Nozik A J 1999 Anti-stokes photoluminescence in colloidal semiconductor quantum dots *Appl. Phys. Lett.* **75** 971
[30] García de Abajo F and Howie A 2002 Retarded field calculation of electron energy loss in inhomogeneous dielectrics *Phys. Rev.* B **65** 115418
[31] García de Abajo F and Howie A 1998 Relativistic electron energy loss and electron-induced photon emission in inhomogeneous dielectrics *Phys. Rev. Lett.* **80** 5180–3
[32] Johnson P B and Christy R W 1972 Optical constants of the noble metals *Phys. Rev.* B **6** 4370–9
[33] Cortie M and Ford M 2007 A plasmon-induced current loop in gold semi-shells *Nanotechnology* **18** 235704
[34] Ross B M and Lee L P 2008 Plasmon tuning and local field enhancement maximization of the nanocrescent *Nanotechnology* **19** 275201
[35] Härtling T, Reichenbach P and Eng L M 2007 Near-field coupling of a single fluorescent molecule and a spherical gold nanoparticle *Opt. Express* **15** 12806–17
[36] Hofmann C E, Javier García de Abajo F and Atwater H A 2011 Enhancing the radiative rate in IIIV semiconductor plasmonic coreshell nanowire resonators *Nano Lett.* **11** 372–6
[37] Stoerzinger K A, Lin J Y and Odom T W 2011 Nanoparticle SERS substrates with 3D Raman-active volumes *Chem. Sci.* **2** 1435–9